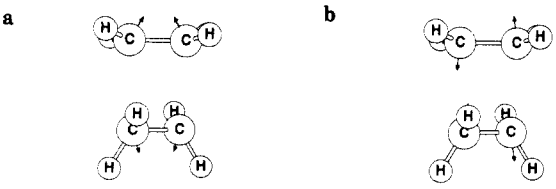

Figure 2. Normal modes corresponding to the two imaginary frequencies for the $2_s + 2_a$ critical point of index 2 for the addition of two ethylene molecules. Only the motion of the carbon atoms is shown: (a) normal mode connecting reactants and products; (b) normal mode connecting two possible gauche transition structures.

fragment (in the case of ethylene, the methylene groups twisted by almost 90°).

The characterization of these critical points by analytical Hessian computation shows that in each case the critical point is a saddle point of index 2. The evolution of the two directions of negative curvature is shown in Figure 2 where we have given the carbon atom components of each normal mode of ethylene + ethylene as an example. Motion along one direction of negative curvature (Figure 2a) leads to the product, while motion along the other direction of negative curvature (Figure 2b) leads to an adjacent gauche transition state, which has been optimized and characterized in all cases. For the ketene + ethylene reaction we have found two different adjacent gauche transition states, one bonded at C1 and the other bonded at C2.

Conclusions

Since each of the supra-antara saddle points is not a true transition structure but rather a local maximum with two directions of negative curvature, the supra-antara reaction pathway does not exist for the examples studied. For the case of ethylene + ethylene and ethylene + oxygen, this might have been expected since the direction of negative curvature that leads to the gauche minimum breaks the symmetry; however, in the case of ketene + ethylene, there is no symmetry. Thus, the results tend to indicate that the supra-antara reaction path may not exist at all for 2 + 2 cycloadditions.

Of course, these computations were carried out with quite modest basis sets. There are numerous examples in the literature where the qualitative nature of a stationary point (see for example ref 9 and 10) was altered by augmenting the basis set with polarization functions. However, for the supra-antara critical points, the second negative direction of curvature (see Figure 2b) connects two gauche fragmentation transition states. A posteriori, it would seem rather unlikely that one could find a maximum (between the supra-antara critical point and the gauche fragmentation transition state) along this coordinate as would be required if the supra-antara critical point were a true transition state.

We do also have some numerical evidence that the qualitative nature of the critical points will not be basis set dependent for these examples. For the ethylene + ethylene example, the very low (>1 kcal/mol) barrier to fragmentation from the trans diradical minimum of tetramethylene appears to be sensitive to the basis set.[8] Doubleday et al.[11] have recently reexamined this problem with a 6-31G* basis. They find that, at the MC-SCF level, the barrier is increased by ca. 1 kcal/mol from the 4-31G [8]/6-31G*[11] result so that the qualitative nature of the critical point does not change in this case.

Registry No. Ethylene, 74-85-1; oxygen, 7782-44-7; ketene, 463-51-4.

(9) Yoshika, Y.; Goddard, J. D.; Schaefer, H. F. *J. Am. Chem. Soc.* **1983**, *105*, 1760.
(10) Saxe, P.; Schaefer, H. F. *J. Chem. Phys.* **1981**, *74*, 1855.
(11) Doubleday, C.; Page, M.; McIver, J. W. *THEOCHEM* **1988**, *163*, 331.

Pseudorotation in Pentacoordinated Phosphorus Compounds. The Influence of the Conformational Transmission Effect on the Barriers to Pseudorotation in Cyclic Alkoxyphosphoranes

A. E. H. de Keijzer,* L. H. Koole, and H. M. Buck

Contribution from the Department of Organic Chemistry, Eindhoven University of Technology, P.O. Box 513, 5600 MB Eindhoven, The Netherlands. *Received September 1, 1987*

Abstract: A variable-temperature ^{13}C NMR study on a series of monocyclic oxyphosphoranes enabled us to examine the influence of the conformational transmission effect on the barriers to pseudorotation in pentacoordinated phosphorus compounds. It is demonstrated that the pseudorotation rate of monocyclic oxyphosphoranes exhibiting the conformational transmission effect is 2-4 times faster as compared to their counterparts in which the effect is absent. It is shown that the conformational change in the basal ligands of the intermediate SP structures, due to the conformational transmission effect, is responsible for the lowering of the activation barriers by 2-3 kJ·mol^{-1}.

Pseudorotation of stable oxyphosphoranes has been the topic of several studies during the past two decades.[1] The polytopal exchange of ligands around pentacoordinated phosphorus has been extensively studied, both because these compounds are presumed to be intermediates in many biological processes involving phosphate esters[2] and especially because of the growing interest in the stereochemistry of reactions of tri- and tetracoordinated phosphorus compounds. These reactions proceed via pentacoordinated phosphorus intermediates, and therefore, the pseudorotation processes may have a great influence on the structure of the reaction products.[3] In the past few years a lot of information has been obtained concerning the influence of the conformational transmission effect on the structure and dynamics

(1) (a) Luckenbach, R. *Dynamic Stereochemistry of Pentacoordinated Phosphorus and Related Elements*; George Thieme Verlag: Stuttgart, 1973. (b) Ramirez, F.; Ugi, I. *Advances in Physical Organic Chemistry*; Academic: London, 1971; Vol. 9, pp 25-126. (c) Hellwinkel, D. *Organic Phosphorus Compounds*; Wiley-Interscience: New York, 1972; Vol. 3, pp 185-339. (d) Holmes, R. R. *Pentacoordinated Phosphorus*; American Chemical Society: Washington, 1980; Vol. 1 and 2, ACS Monograph No. 175 and 176. (e) Emsley, J.; Hall, D. *The Chemistry of Phosphorus*; Harper & Row: New York, 1976.

(2) Benkovics, S. J.; Schray, K. J. *The Enzymes*, 3rd ed.; Academic: New York; 1973; Vol. VII, Chapter 6.
(3) Trippett, S. *Phosphorus Sulfur* **1976**, *1*, 89.

0002-7863/88/1510-5995$01.50/0

Table I. ^1H NMR and ^{31}P NMR Data for the Phosphoranes **1–3** at 25 °C

	^1H[a]	CH_3	$COCH_3$	$POCH_2$[b]	H_4	C_6H_5	$H_{2'}/H_{3'}$	$H_{1'}/H_{4'}$	$C(CH_3)_2$	XCH_3	X	$H_{2'}$	OCH_2CH_3	$COCH_2$	^{31}P[c]
1		1.84	2.47	3.64	4.13	7.20									−27.1
2a		1.84	2.44	3.64	4.12	7.17–7.28	1.53	1.53			1.53				−29.2
2b		1.86	2.45	3.62–3.92	4.15	7.18–7.30	1.80	3.62–3.92							−28.4[d]
2c		1.74	2.22	3.60–3.95			1.58	1.58	1.46		1.58				−29.7
2d		1.92	2.26	3.68–4.20			1.90	3.68–4.20	1.46						−28.8
3a		1.67	2.47	3.70	4.15	6.77–7.23				0.73	1.27	1.27			−29.3
3b		1.67	2.47	3.78	4.18	6.97–7.37				3.07		3.20			−29.1
3c		2.15		3.63					1.53	0.73	1.32	1.32	0.97	3.93	−25.6
3d		2.11		3.77					1.52	3.07		3.23	0.96	3.90	−25.7

[a] ^1H NMR recorded at 300 MHz in $CDCl_3$ with TMS as internal standard for the compounds **1** and **2**, while phosphoranes **3** were measured at 200 MHz in $C_6D_5CD_3$ solvent. [b] The $POCH_2$ signals of compounds **1–3** were broadened by slow exchange at room temperature. [c] ^{31}P NMR was performed in $CDCl_3$ with 85% H_3PO_4 as external standard at 36.4 MHz for **1** and **2**, while phosphoranes **3** were measured at 80.9 MHz in $C_6D_5CD_3$ solvent. Downfield shifts are designated as positive. [d] In acetone-d_6 the spectrum shows four signals in the approximate ratio 1:2:2:1 at −24.8, −24.9, −25.0, and −25.1 ppm.

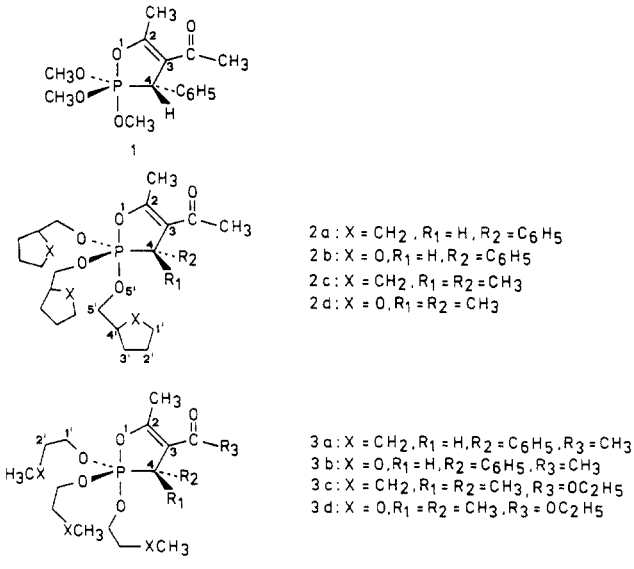

Figure 1. Model compounds **1**, **2**, and **3** studied in this work.

of pentacoordinated phosphorus compounds.[4] In the present work we studied quantitatively the contributions of the conformational transmission effect to the activation barrier of the multiple pseudorotation processes in a series of monocyclic oxyphosphoranes. We thus examined the isomerization processes of the phosphoranes **2a–d** and **3a–d** which are closely related to phosphorane **1** (Figure 1), first prepared by Ramirez and his co-workers.[5] In this compound the pseudorotation pathways have been extensively studied and are now well-defined.[6]

The $POCH_2$ moieties of compounds **2** and **3** exhibit an exchange process that can be readily followed by variable-temperature ^{13}C NMR and allows the determination of the activation barriers associated with the isomerization process. The activation barriers of the pseudorotation process of the compounds containing X = CH_2 (**2a**, **2c**, **3a**, and **3c**) were compared with those of the phosphoranes where X = O (**2b**, **2d**, **3b**, and **3d**). Hence, some conclusions about the influence of the conformational transmission effect on the magnitude of the pseudorotation barriers could be drawn.[7]

Results and Discussion

Exchange Process Studies. In order to examine the reliability of the ^{13}C variable-temperature investigations, phosphorane **1** was selected as a reference system. The ^1H NMR low-temperature behavior of this compound has now been well-established.[6] The results obtained for compound **1** in the present study, as well as data on other phosphoranes presented in previous studies,[6f,8] clearly demonstrate the usefulness of ^{13}C NMR investigations concerning exchange processes in P(V) trigonal-bipyramidal (TBP) phosphoranes. The spectral parameters of compounds **1**, **2**, and **3** are listed in Tables I and II, respectively.

At 40 °C the three oxamethylene carbons of compound **1** appear as a doublet, the signal is split by ^{31}P with J_{PC} = 13 Hz, indicating a fast pseudorotation process. At about 25 °C the doublet collapses to a broad band, and at about −30 °C this band is again resolved. At −45 °C the spectrum shows three partially separated doublets, corresponding to one axial and two equatorial methoxy groups. The upfield doublet must be assigned to the axial group, while the two downfield doublets then correspond to the two diastereotopic equatorial methoxy groups, since they differ in their relationship to the phenyl ring.[6a] Obviously, at this temperature the structure of **1** is frozen and pseudorotation is inhibited. The $\Delta G^{\ddagger}$ for this isomerization process amounts to 51.3 kJ·mol^{-1}, which is in good agreement with the 51.0 kJ·mol^{-1} reported by Gorenstein.[6c] The results of the ^{13}C NMR studies on compounds **1**, **2**, and **3** are summarized in Table III.

The activation parameters of the exchange process have been evaluated from the computer simulation of the experimental spectra at different temperatures[9] (Figure 2) by analyzing the

(4) (a) Koole, L. H.; Lanters, E. J.; Buck, H. M. *J. Am. Chem. Soc.* **1984**, *106*, 5451. (b) Koole, L. H.; van Kooyk, R. J. L.; Buck, H. M. *J. Am. Chem. Soc.* **1985**, *107*, 4032. (c) de Vries, N. K.; Buck, H. M. *Recl. Trav. Chim. Pays-Bas* **1986**, *106*, 150. (d) de Vries, N. K.; Buck, H. M. *Phosphorus Sulfur* **1987**, *31*, 267. (e) van Genderen, M. H. P.; Koole, L. H.; Olde Scheper, B. G. C. M.; van de Ven, L. J. M.; Buck, H. M. *Phosphorus Sulfur* **1987**, *32*, 73. (f) van Genderen, M. H. P.; Buck, H. M. *Recl. Trav. Chim. Pays-Bas* **1987**, *106*, 449. (g) van Genderen, M. H. P.; Buck, H. M. *Magn. Reson. Chem.* **1987**, *25*, 872. (h) de Keijzer, A. E. H.; Buck, H. M. *Phosphorus Sulfur* **1987**, *31*, 203.

(5) Ramirez, F.; Madan, O. P.; Heller, S. R. *J. Am. Chem. Soc.* **1965**, *87*, 731.

(6) (a) Gorenstein, D.; Westheimer, F. H. *J. Am. Chem. Soc.* **1967**, *89*, 2762. (b) Gorenstein, D.; Westheimer, F. H. *J. Am. Chem. Soc.* **1970**, *92*, 634. (c) Gorenstein, D. *J. Am. Chem. Soc.* **1970**, *92*, 644. (d) Holmes, R. R. *J. Am. Chem. Soc.* **1978**, *100*, 433. (e) Buono, G.; Llinas, J. R. *J. Am. Chem. Soc.* **1981**, *103*, 4532. (f) Aganov, A. V.; Polezhaeva, N. A.; Khayanov, A. I.; Arbuzov, B. A. *Phosphorus Sulfur* **1985**, *22*, 303. (g) Kay, P. B.; Trippett, S. *J. Chem. Soc., Chem. Commun.* **1985**, 135.

(7) One of the referees suggested a zwitterionic hexacoordinated phosphorus transition state to account for the more rapid pseudorotation rates in case of the compounds with X = O. We have determined the pseudorotation barriers of two compounds (**a**, **b**) in which no conformational transmission is present, but in which there are still tetrahydrofuran oxygens present, thus permitting a zwitterionic transition state to accelerate the pseudorotation. The

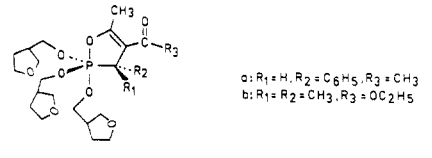

pseudorotation barriers, 55.2 ± 0.4 and 71.9 ± 0.8 kJ·mol^{-1}, respectively, are in excellent agreement with those found for the cyclopentyl compounds **2a** and **2c**. Therefore we conclude that there is no involvement of a hexacoordinated zwitterionic phosphorus transition state in the compounds investigated in the present study. Full experimental data regarding the syntheses and ^{13}C variable temperature measurements of these compounds will be published elsewhere.

(8) (a) van Ool, P. J. J. M; Buck, H. M. *Recl. Trav. Chim. Pays-Bas* **1983**, *102*, 215. (b) van Ool, P. J. J. M.; Buck, H. M. *Recl. Trav. Chim. Pays-Bas* **1984**, *103*, 119.

(9) Sandström, J. *Dynamic NMR Spectroscopy*; Academic: London, 1982.

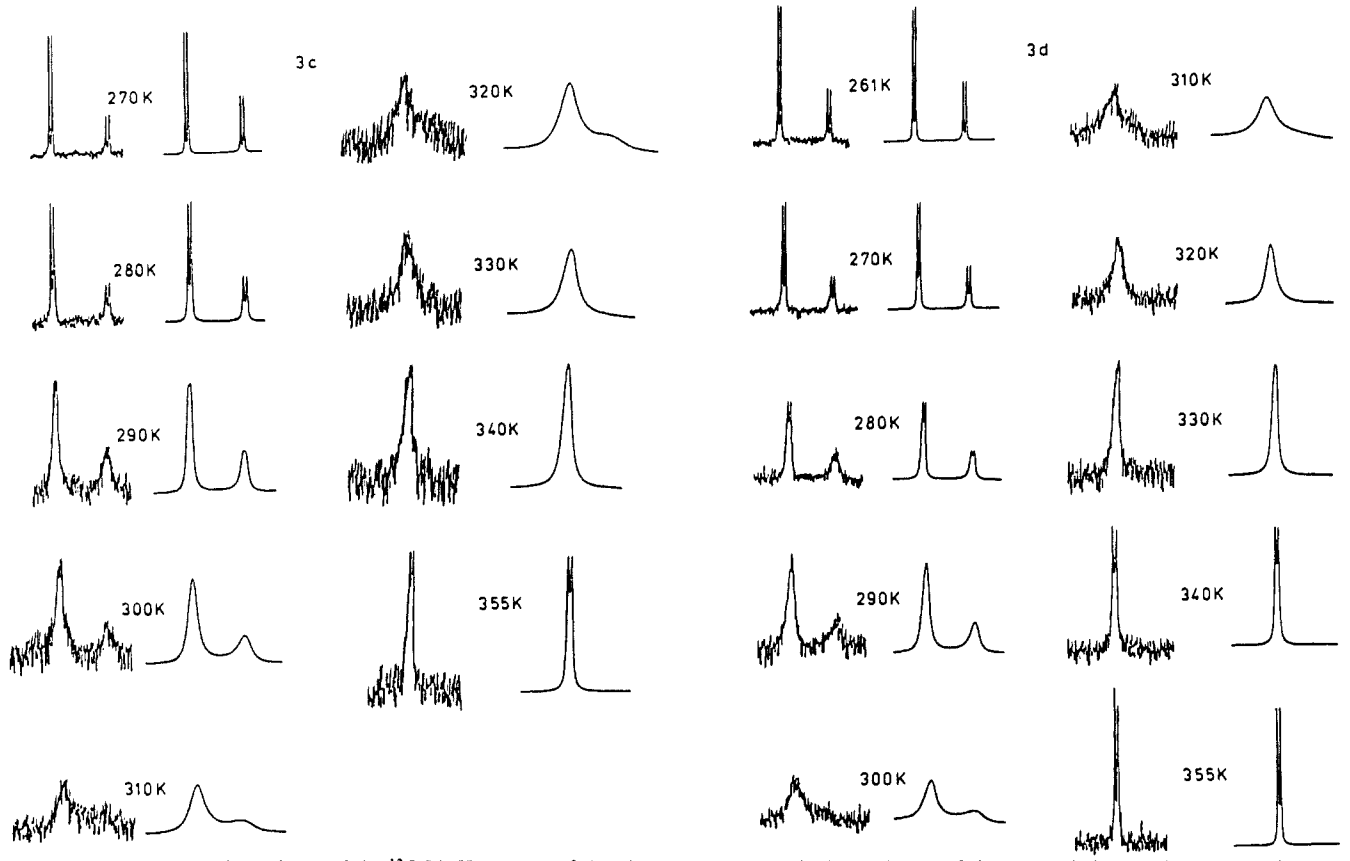

Figure 2. Temperature dependence of the ^{13}C NMR spectra of the phosphoranes **3c** and **3d**. Exchange of the oxamethylene carbons. Experimental (left) and calculated (right) spectra at different temperatures.

coupled ABX two-site exchange with $J_{AB} = 0$, using the DNMR/3 program.[10]

From the results reported in Table III we may conclude that the activation barrier $\Delta G^{\ddagger}$ for phosphoranes containing the same oxaphospholene ring is dependent upon the nature of the atom X in the alkyloxy ligands. Comparing the results for the compound-pairs **2a–2b**, **2c–2d**, **3a–3b**, and **3c–3d** reveals a small but distinct difference in $\Delta G^{\ddagger}$, between the two types of compounds. In all cases where X is oxygen, a lowering of the activation barrier was observed as compared to the corresponding phosphoranes with $X = CH_2$. The resulting difference in pseudorotation rates can be expressed as $k(O)/k(CH_2)$ and is included in Table III. Examining these data we conclude that the phosphoranes containing X = O show a ligand exchange rate that is 2–4 times faster as compared to the compounds with $X = CH_2$. To be able to explain this phenomenon in terms of the contribution of the conformational transmission effect to the barrier of pseudorotation,[7] we must take a closer look at the possible isomerization pathways.

Isomerization Pathways. Different isomerization pathways describe the ligand exchange process. These interconversion pathways may be topologically depicted by the diagram[11] as shown in Figure 3. The TBP topomers are associated with vertices and the transformation pathways with edges. Berry pseudorotation[12] (BPR) and turnstile rotation[13] (TR) mechanisms belonging to the same rearrangement mode are permutationally indistinguishable. Hence, every edge represents either BPR or TR mechanisms with the respective transition state proper to these mechanisms.

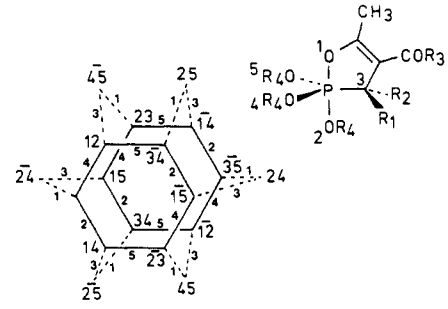

Figure 3. Topological diagram for pseudorotation, summarizing isomerization (solid lines) and epimerization (dashed lines) processes for compounds **1**, **2**, and **3**. Isomers are denoted by Gielen's notation.[11]

However, on the basis of both theoretical estimates[14,15] and solid-state structural distortions,[16] the BPR process seems to be the most likely. Therefore we will not consider the TR process in the following discussions.

Thus, (a) excluding topomers '**13**' and '$\overline{13}$' because the oxaphospholene ring is unable to occupy the two axial positions of a TBP, (b) not taking into consideration any epimerization pro-

(10) Kleier, D. A.; Binsch, G. *DNMR/3*; Quantum Chemistry Program Exchange No. 165; Indiana University, 1969.

(11) Gielen, M. *Chemical Applications of Graph Theory*; Academic: New York, 1976; pp 261–298.

(12) The BPR mechanism involves the simultaneous bending of a pair of equatorial and a pair of axial bonds, causing the formation of an intermediate square pyramidal structure (SP) on the way to the interconverted TBP, see: Berry, R. S. *J. Chem. Phys.* **1960**, *32*, 933.

(13) Ugi, I.; Ramirez, F.; Marquarding, D.; Klusacek, H.; Gokel, G.; Gillespie, P. *Angew. Chem.* **1970**, *82*, 766.

(14) (a) Strich, A.; Veillard, A. *J. Am. Chem. Soc.* **1973**, *95*, 5574. (b) Hoffmann, R.; Howell, J. M.; Muetterties, E. L. *J. Am. Chem. Soc.* **1972**, *94*, 3047. (c) Russegger, P.; Brickmann *Chem. Phys. Lett.* **1975**, *30*, 276. (d) Russegger, P.; Brickmann *J. Chem. Phys.* **1975**, *62*, 1086. (e) Gillespie, P.; Hoffmann, R.; Klusacek, H.; Marquarding, D.; Pfohl, S.; Ramirez, F.; Tsolis, E. A.; Ugi, I. *Angew. Chem., Int. Ed. Engl.* **1971**, *10*, 687.

(15) (a) Bernstein, L. S.; Abramowitz, S.; Levin, I. W. *J. Chem. Phys.* **1976**, *64*, 3228. (b) Bernstein, L. S.; Kim, J. J.; Pitzer, K. S.; Abramowitz, S.; Levin, I. W. *J. Chem. Phys.* **1975**, *62*, 3671. (c) Altmann, J. A.; Yates, K.; Csizmadia, I. G. *J. Am. Chem. Soc.* **1976**, *98*, 1450. (d) Rauk, A.; Allen, L. C.; Mislow, K. *J. Am. Chem. Soc.* **1972**, *94*, 3035. (e) Shih, S. K.; Peyerinhoff, S. D.; Buenker, R. J. *J. Chem. Soc., Faraday Trans. II* **1979**, *75*, 379.

(16) (a) Holmes, R. R.; Deiters, J. A. *J. Chem. Res.* **1977**, 92. (b) Holmes, R. R.; Deiters, J. A. *J. Am. Chem. Soc.* **1977**, *99*, 3318. (c) Holmes, R. R. *Acc. Chem. Res.* **1979**, *12*, 257. (d) Buono, G.; Llinas, J. R. *J. Am. Chem. Soc.* **1981**, *103*, 4532.

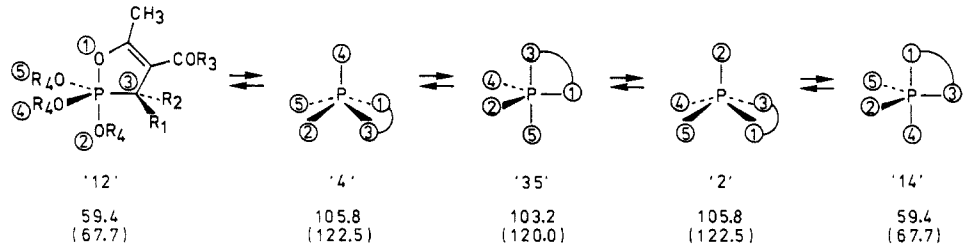

Figure 4. Isomerization pathway for the phosphoranes **1–3**. The bold numbers associated with each structure identify the isomer on the topological diagram of Figure 3. The relative isomer energy, in kJ·mol^{-1}, for compounds **1**, **2a**, **2b**, **3a**, **3b** (R_1 = H, R_2 = C_6H_5) and **2c**, **2d**, **3c**, **3d** (R_1 = R_2 = CH_3; in parentheses) estimated from Holmes' model[6] is indicated.

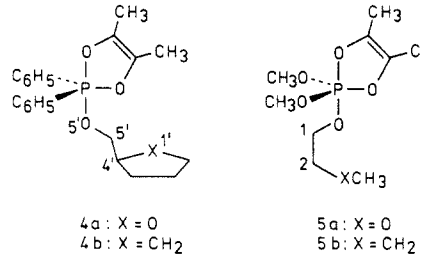

Figure 5. Model compounds **4** and **5**.

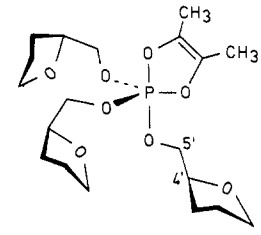

Figure 6. Model compound **6**, dominant C_4–$C_{5'}$ rotamers are drawn for the tetrahydrofurfuryl ligands.

cesses involving the high-energy topomers '**24**', '**45**', '**25**', '$\overline{24}$', and '$\overline{25}$', in which the oxaphospholene ring is forced to span an unfavored diequatorial position in the TBP, such intermediates would require a barrier[6] of at least 80 kJ·mol^{-1}, and (c) taking into account the fact that the two types of pathways

$$\text{'12'} \overset{5}{\rightleftarrows} \text{'34'} \overset{2}{\rightleftarrows} \text{'15'} \overset{4}{\rightleftarrows} \text{'23'} \overset{5}{\rightleftarrows} \text{'14'} \quad (1)$$

$$\text{'12'} \overset{4}{\rightleftarrows} \text{'35'} \overset{2}{\rightleftarrows} \text{'14'} \quad (2)$$

are indistinguishable because of the use of one kind of alkyloxy ligand only, we may conclude that the interconversion of the ground-state TBP proceeds via one TBP and two square-pyramidal (SP) transition states as is described in (2). Figure 4 depicts the low-energy isomerization pathway for the phosphoranes **1**, **2**, and **3**, with their TBP and SP intermediates.

Interpretation of the Energy Barriers. From the experimental $\Delta G^{\ddagger}$ values of exchange processes occurring in a variety of different phosphoranes, Holmes[6d] has established a reliable[17] model for the relative energies of all possible TBP and SP stereoisomers on the isomerization pathway. Particularly, the family of compounds closely resembling phosphorane **1** was studied extensively, which enables us to use this model without further restraint. In the pathway shown in Figure 4, the topomer '**35**' is energetically close to the neighboring SP structures '**2**' and '**4**'. The energy difference Δ(SP–TBP) amounts to 2.6 kJ·mol^{-1}. Therefore, we may conclude that the isomerization in phosphoranes **1**, **2**, and **3** takes place by way of the SP transition state. It is well-known, both from reported calculations[1d,14b,15c,18] as well as from our own MNDO calculations[19] on pentacoordinated phosphorus compounds, that the apical position in the SP has properties that are comparable with the equatorial positions in a TBP. Similarly the basal ligands in the SP correspond closely in properties to the axial groups in a TBP. Recent 300-MHz ^{1}H NMR studies[4a] on a set of 5′-P(IV) and 5′-P(V) TBP tetrahydrofurfuryl and cyclopentylmethyl model compounds **4** (Figure 5), as well as a 300- and 500-MHz ^{1}H NMR study on the solvent polarity effects upon these model compounds,[4b] revealed a conformational transmission effect in the C_4–$C_{5'}$ bond of the axial tetrahydrofurfuryl moiety.

It was confirmed that the enhanced charge repulsion between the $O_{5'}$ and $O_{1'}$ in the axial ligand of the TBP results in a rotation around the C_4–$C_{5'}$ bond, thus prompting the axial ligand to adopt a g^- conformation.[22a] From an additional study[4e] involving the phosphoranes **5** it was also deduced that this conformational transmission effect[22b] occurs in the axis of the TBP. The relevant data of these investigations, the dominant rotamer populations adopted by the alkyloxy moieties in the equatorial and axial positions of the TBP structures, respectively, are collected in Table IV.

The low-temperature study[4a] of model compound **6** (Figure 6) enabled us to obtain the enthalpy and entropy parameters con-

(17) McDowell, R. S.; Streitwieser, A., Jr. *J. Am. Chem. Soc.* **1985**, *107*, 5849.

(18) (a) Deiters, J. A.; Gallucci, J. C.; Clark, Th. E.; Holmes, R. R. *J. Am. Chem. Soc.* **1977**, *99*, 5461. (b) Marsden, C. J. *J. Chem. Soc., Chem. Commun.* **1984**, 401.

(19) MNDO calculations were performed with the MNDO program (QCPE version)[20] which does not include d-orbital functions for phosphorus. A number of ab initio studies on P(V) compounds,[21] however, revealed that the principal concepts of bonding are adequately described without the introduction of d-functions for phosphorus. Compound **1** was selected to calculate the P–O bond lengths and the electron densities on the oxygen atoms in both TBP and SP structures. To simplify the calculations without changing the actual structures, the substituents of the oxaphosphole ring were replaced by hydrogen atoms. The structures were fully optimized with respect to all bond lengths, bond angles, and twist angles except those required to preserve the basic TBP and SP geometries. The calculations for the TBP structure revealed a P–O_{axial} and P–$O_{equatorial}$ bond length of 1.67 and 1.63 Å, respectively. The electron densities for O_{axial} and $O_{equatorial}$ were −0.59 and −0.52, respectively. For the SP structure P–O_{apical} was calculated to be 1.61 Å, with an electron density of −0.51 on O_{apical}. The basal oxygens possess an electron density of −0.53 and −0.55 and a P–O_{basal} bond length of 1.65 Å.

(20) Dewar, M. J. S. *J. Am. Chem. Soc.* **1977**, *99*, 4899.

(21) Janssen, R. A. J.; Visser, G. J.; Buck, H. M. *J. Am. Chem. Soc.* **1984**, *106*, 3429.

(22) (a) In solution a rapid interconversion between the three staggered conformations g^+, g^t, and g^- exists. The rotamer populations can be obtained,[4a]

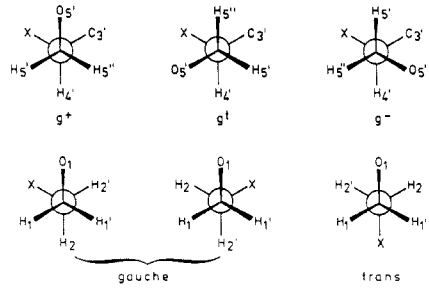

using the empirically generalized Karplus relation developed by Altona et al.[23] (b) The conformation around the C_1–C_2 bond of phosphoranes **5** is also an equilibrium between staggered rotamers, but as two of these rotamers are mirror images and have identical populations, a two-state description with a gauche and a trans state is used. The population densities of these rotamers have been determined from the vicinal proton–proton coupling constants[4d] of the C_1–C_2 fragment.

(23) Haasnoot, C. A. G.; de Leeuw, F. A. A. M.; Altona, C. *Tetrahedron* **1980**, *36*, 2783.

Table II. ^{13}C NMR Data for the Phosphoranes **1–3** at 25 °C

$^{13}C^a$	CH_3	$C(CH_3)_2$	$C_{1'}$	$C_{2'}$	$C_{3'}$	$C_{4'}$	X	XCH_3	$COCH_3$	POC[b]	C_2	C_3	C_4	C_6H_5[c]	C=O	$COCH_2$	OCH_2CH_3	solvent
1	15.8								28.0	53.8	163.5	112.0	47.1	125.0–129.0 138.3	165.1			CD_2Cl_2
2a	15.9		24.3	24.3	27.8	39.3	27.8		28.0	70.0	137.0	111.8	47.8	125.0–129.5 138.0	165.0			CD_2Cl_2
2b	15.6		66.8	24.4	26.5	76.5			28.0	68.0	137.8	112.3	47.3	125.8–128.8 139.8	168.5			CD_2Cl_2
2c	19.0	23.5	26.2	26.2	29.9	36.4	29.9		29.9	68.5 (a) 72.5 (e)	163.5	120.5	43.8		193.8			C_6D_5Br
2d	18.5	23.7	68.3	24.4	26.5	77.5			29.9	67.4 (a) 70.3 (e)	163.4	120.4	43.8		194.0			C_6D_5Br
3a	17.7			33.7			19.9	14.4	29.9	67.5	166.5	113.5	49.5	127.0–130.5 139.0	194.0			$C_6D_5CD_3$
3b	17.9			73.0				59.0	30.1	67.3	166.5	114.0	49.8	127.0–130.0 139.0	194.0			$C_6D_5CD_3$
3c	18.0	24.5					19.9	14.8		68.2 (a) 64.2 (e)	164.1	109.6	43.0		166.9	59.4	15.3	$C_6D_5CD_3$
3d	17.8	24.5	73.5					59.0		67.7 (a) 63.9 (e)	164.0	109.5	43.3		167.0	17.8	15.5	$C_6D_5CD_3$

[a] The spectra of compounds **1** and **2** were recorded at 75.3 MHz, while the phosphoranes **3** were measured at 50.3 MHz. [b] Compounds **2c**, **2d**, **3c**, and **3d** show no pseudorotation at 25 °C, signal intensities are approximately (a):(e) = 1:2. (a) = axial, (e) = equatorial. [c] Downfield aromatic signal is designated to the ipso-carbon of the phenyl ring.

cerning the equilibria $g^- \rightleftarrows g^+$ and $g^- \rightleftarrows g^t$. The results of the study are summarized in Table V.

From Table V we can deduce that at the coalescence temperature the net energy gain for a $g^t/g^+ \rightarrow g^-$ transition will be approximately 2–4 kJ·mol^{-1}. With Holmes' theory and the data presented above it is now possible to explain the difference in $\Delta G^{\ddagger}$ values between the two types of phosphoranes studied in this work.

In the phosphoranes **2a**, **2c**, **3a**, and **3c**, containing a methylene group (X = CH_2) in the alkyloxy ligand, the isomerization pathway is essentially the same as is depicted in Figure 4 (vide supra). The SP structure determines the magnitude of the activation barrier in the BPR process. In case the phosphoranes contain an additional oxygen atom in the alkyloxy ligand (**2b**, **2d**, **3b**, and **3d**, X = O), the actual energies of the topomers in the pseudorotation pathway will be different. Starting with the ground-state TBP ('**12**' in Figure 4, vide supra) the alkyloxy ligands occupy one axial and two equatorial positions. The equatorial ligands possess a g^+/g^t conformation (Table IV, vide supra), and it has been demonstrated that the enhanced charge density on the axial $O_{5'}$ atom in the TBP structure is partially accommodated by the conformational change in the axial alkyloxy ligand toward the more stable g^- conformer. The same situation is encountered in the transition-state TBP ('**35**', Figure 4). There is, however, no net change in energy difference between these structures because both TBP structures contain the same number of axial and equatorial alkyloxy ligands. The situation is somewhat different in the SP transition states '**2**' and '**4**' (Figure 4). From the data regarding the conformational transmission effect in the axis of the TBP and the comparability of the basal positions in the SP structure with the axial positions in a TBP, we can conclude that in the SP transition state the enhanced charge density on the basal oxygen atoms will now be accommodated by *two* alkoxy g^- conformers, thus resulting in a net stabilization of this topomer as compared to both the TBP ground and transition states. As a result there will be a decrease in $\Delta G^{\ddagger}$ of the pseudorotation process.

Holmes' theory predicts the TBP transition state to be 2.6 kJ·mol^{-1} lower in energy than the SP transition states. The experimental data regarding the energy effect of a $g^+/g^t \rightarrow g^-$ transition, which takes place in the SP structures, show a net energy effect of 2–4 kJ·mol^{-1}. Hence it follows that, because the topomers '**2**' and '**4**' are energetically very close to the neighboring TBP structure '**35**', the TBP transition state will now become the highest energy state that has to be traversed in the isomerization process. The energy changes caused by the conformational transmission effect have been visualized in Figure 7.

Using this theoretical approach, we are now able to predict a lowering of the activation barrier of the pseudorotation process in the phosphoranes exhibiting the conformational transmission effect, as compared to the corresponding phosphoranes in which the conformational transmission effect is absent. It can be deduced that the difference in $\Delta G^{\ddagger}$ will amount to about 2–3 kJ·mol^{-1}. The experimental results presented in Table III (vide supra) indeed show that the $\Delta G^{\ddagger}$ values of the phosphoranes **2a**, **2c**, **3a**, and **3c** exceed the activation barriers of their counterparts, exhibiting the conformational transmission effect, by 1.8–3.4 kJ·mol^{-1}. Therefore we may conclude that the experimental results are in excellent agreement with the theoretical considerations presented above.

Concluding Remarks

This study clearly demonstrates the contribution of the conformational transmission effect to the barriers of pseudorotation in monocyclic oxyphosphoranes. It clearly shows that the conformational transmission effect plays an important role in the actual isomerization pathways of the phosphoranes studied. Phosphoranes **2a**, **2c**, **3a**, and **3c** proceed through a high-energy SP transition state comparable with the SP transition state in phosphorane **1**. The isomerization in the corresponding phosphoranes **2b**, **2d**, **3b**, and **3d**, exhibiting the conformational transmission effect, however, takes place by way of a low-energy TBP transition state. The results are in excellent agreement with both theoretical estimations and experimental data obtained from

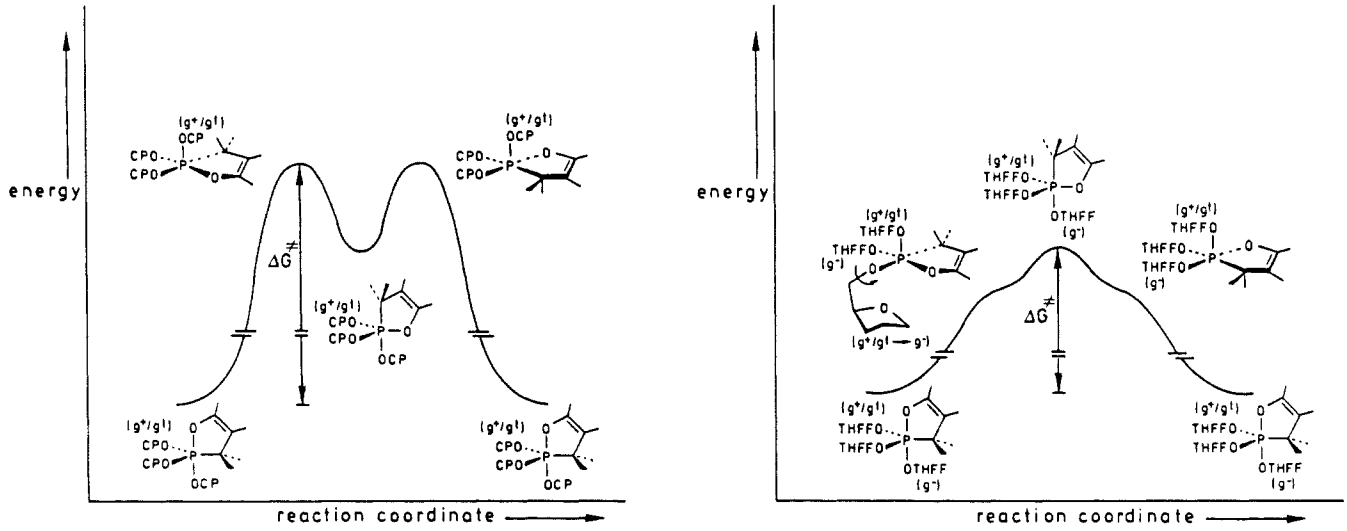

Figure 7. Influence of the conformational transmission effect upon the energy of the SP topomers and the $\Delta G^{\ddagger}$ of the pseudorotation process. CP = cyclopentylmethyl and THFF = tetrahydrofurfuryl.

Table III. Activation Parameters for the Exchange Processes in the Phosphoranes **1–3**

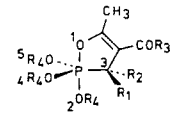

	R_1	R_2	R_3	R_4[a]	solvent	T_c[b]	$\Delta\nu$[c]	$\Delta G^{\ddagger}$[d]	$\Delta G^{\ddagger}$[e]	k_O/k_C[f]
1	H	C_6H_5	CH_3	CH_3	CD_2Cl_2	271	320	51.3	51.0	
2a	H	C_6H_5	CH_3	CP	CD_2Cl_2	288	325	54.6	54.6	4.1
2b	H	C_6H_5	CH_3	THFF	CD_2Cl_2	270	295	51.2	51.0	
2c	CH_3	CH_3	CH_3	CP	C_6D_5Br	371	285	71.5	71.6	2.1
2d	CH_3	CH_3	CH_3	THFF	C_6D_5Br	358	216	69.7	69.8	
3a	H	C_6H_5	CH_3	C_4H_9	$C_6D_5CD_3$	275	231	52.8	52.7	2.1
3b	H	C_6H_5	CH_3	$C_2H_4OCH_3$	$C_6D_5CD_3$	265	201	51.0	51.2	
3c	CH_3	CH_3	OC_2H_5	C_4H_9	$C_6D_5CD_3$	328	202	63.8	63.9	3.2
3d	CH_3	CH_3	OC_2H_5	$C_2H_4OCH_3$	$C_6D_5CD_3$	313	182	61.0	61.1	

[a] CP = cyclopentylmethyl, THFF = tetrahydrofurfuryl. [b] The coalescence temperatures T_c (K) refer to the temperatures of maximum broadening of the NMR signals and were determined with an accuracy of ±2 K. [c] Differences in chemical shifts (Hz) between the equatorial and the axial sites in the absence of exchange, measured with an accuracy of ±2 Hz. [d] $\Delta G^{\ddagger}$ values (kJ·mol^{-1}) calculated from the equation $\Delta G^{\ddagger} = (1.91 \times 10^{-2}) T_c(9.973 + \log (T_c/\Delta\nu))$. Calculated errors lie within ±0.4 kJ.mol^{-1}. [e] Calculated from the equation $\Delta G_c^{\ddagger} = \Delta H^{\ddagger} - T_c\Delta S^{\ddagger}$, whereas the activation parameters have been evaluated from a least-squares plot of ln (k/T) vs $1/T$. Estimated uncertainty ±0.5 kJ.mol^{-1}. [f] Rate constant ratio for the pseudorotation velocities, comparing compounds with X = O and X = CH_2, respectively. Ratios were calculated from the equation $RT \ln (k_O/k_C) = \Delta G^{\ddagger}(CH_2) - \Delta G^{\ddagger}(O)$ at 20 °C.

Table IV. Dominant Rotamer Populations[22] for Axial and Equatorial Alkyloxy Moieties in Phosphoranes **4** and **5**

	equatorial	axial
4a	g^+/g^t	g^-
4b	g^t/g^-	g^t/g^-
5a[a]	g	g/t
5b[a]	g/t	g/t

[a] The conformation around the C_1–C_2 bond of these phosphoranes is an equilibrium between three staggered rotamers, but as two of these are mirror images and have identical populations, a two-state description with a gauche (=g^+/g^t) and a trans state (=g^-) is used.

Table V. Thermodynamic Parameters of the C_4–$C_{5'}$ Conformational Equilibria for Axial and Equatorial Tetrahydrofuryl Ligands in **6**

	axial	equatorial
$\Delta H°(g^- \rightarrow g^+)$	4.7 kJ·mol^{-1}	−4.3 kJ·mol^{-1}
$\Delta S°(g^- \rightarrow g^+)$	7.2 J·mol^{-1}·K^{-1}	−9.8 J·mol^{-1}·K^{-1}
$\Delta H°(g^- \rightarrow g^t)$	6.1 kJ·mol^{-1}	−4.0 kJ·mol^{-1}
$\Delta S°(g^- \rightarrow g^t)$	6.9 J·mol^{-1}·K^{-1}	−8.4 J·mol^{-1}·K^{-1}

studies concerning the conformational transmission effect.

Experimental Section

Spectroscopy. ^{1}H NMR spectra were run in the FT mode at 300 MHz on a Bruker CXP-300 for compounds **1** and **2** and at 200 MHz on a Bruker AC-200 for compound **3**. Proton chemical shifts are referenced against TMS as internal standard. ^{31}P NMR spectra were run in the FT mode at 36.4 MHz on a Bruker HX-90R with a Digilab FT-NMR-3 pulsing accessory (compounds **1** and **2**) and at 80.9 MHz on a Bruker AC-200 (compound **3**). Chemical shifts are related to 85% H_3PO_4 as external standard and are designated positive if downfield with respect to the reference. ^{13}C NMR spectra were recorded in the FT mode at 75.3 MHz on a Bruker CXP-300 (compounds **1** and **2**) and at 50.3 MHz on a Bruker AC-200 (compound **3**).

Chemical shifts are referenced against internal TMS. The variable-temperature ^{13}C spectra were obtained by using a Bruker B-VT 1000 variable-temperature unit, ensuring an error in temperature measurement within ±1 °C.

Synthesis. All solvents and commercial reagents were reagent grade and were dried by conventional methods before use. All moisture-sensitive compounds were handled under a dry nitrogen atmosphere. Trimethyl and tributyl phosphite were purchased from Janssen Chimica and were purified by distillation before use. The general instability of the phosphites and oxyphosphoranes has precluded the obtention of standard analytical data. The identification of these compounds rests therefore on ^{1}H, ^{13}C, and ^{31}P spectroscopy, methods of preparation, and comparison of the obtained data with those presented for well-defined P(III) and P(V) compounds.[5,6]

Tris(tetrahydrofurfuryl) Phosphite. This compound was prepared from tetrahydrofurfuryl alcohol and PCl_3 according to the procedure described by Koole et al.[4a] Bp: 140–142 °C (0.002 mmHg). Yield: 74%. ^{1}H NMR ($CDCl_3$): δ 1.60–2.20 (m, 12 H, H(3′)/H(4′)),

3.45–4.25 (m, 15 H, H(1′)/H(2′)/$POCH_2$). ^{13}C NMR (C_6D_5Br): δ 26.0 (C(2′)), 28.3 (C(3′)), 64.7 (C(4′)), 68.3 (C(1′)), 78.2 ($POCH_2$). ^{31}P NMR ($CDCl_3$): δ 139.0.

Tris(cyclopentylmethyl) Phosphite. To a stirred and cooled (0 °C) solution of cyclopentylmethyl alcohol (40.8 g; 408 mmol) and triethylamine (41.2 g; 408 mmol) in 600 mL of anhydrous diethyl ether was added dropwise a solution of PCl_3 (18.7 g; 136 mmol) in 100 mL of anhydrous diethyl ether. After completion of the addition, the mixture was stirred for 0.5 h at room temperature and refluxed for 1 h. The precipitated triethylamine hydrochloride was removed by filtration. After removal of the solvent the oily residue was distilled under reduced pressure affording the desired product as a colorless liquid. Bp: 148 °C (0.01 mmHg). Yield: 62%. ^1H NMR ($CDCl_3$): δ 1.30–1.85 (m, 27 H, H(1′)/H(2′)/H(3′)/H(4′)/X), 3.70 (t, 6 H, $POCH_2$). ^{13}C NMR (C_6D_5Br): δ 25.7 (C(1′)/C(2′)), 29.5 (C(3′)/X), 41.0 (C(4′)), 66.0 ($POCH_2$). ^{31}P NMR ($CDCl_3$): 139.1.

Tris(2-methoxyethyl) Phosphite. This compound was prepared from 2-methoxyethanol and PCl_3 according to the procedure described for the preparation of tris(cyclopentylmethyl) phosphite. Bp: 83 °C (0.25 mmHg). Yield: 65%. ^1H NMR ($C_6D_5CD_3$): δ 3.25 (s, 3 H, OCH_3), 3.43 (t, 2 H, OCH_2), 3.96 (dt, 2 H, $POCH_2$). ^{13}C NMR ($C_6D_5CD_3$): δ 58.5 (OCH_3), 61.5 ($POCH_2$), 72.6 (OCH_2). ^{31}P NMR ($C_6D_5CD_3$): δ 139.8.

3-(Phenylmethylene)-2,4-pentanedione was prepared from benzaldehyde and 2,4-pentanedione according to a literature procedure.[24] Bp: 168–170 °C (13 mmHg). Yield: 73%. ^1H NMR ($CDCl_3$): δ 2.23 (s, 3 H, $COCH_3$), 2.38 (s, 3 H, $COCH_3$), 7.27 (m, 5 H, Ar), 7.37 (s, 1 H, CH). ^{13}C NMR (CD_2Cl_2): δ 25.5 ($COCH_3$), 30.9 ($COCH_3$), 128.3–130.0 (phenyl), 132.5 (ipso), 138.9 (C=C), 144.9 (C=C), 200.4 (C=O). Anal. Calcd for $C_{12}H_{12}O_2$: C, 76.57; H, 6.43. Found: C, 77.05; H, 6.53. MS, *m/e* 188.15 (M^+; calcd 188.23).

3-(1-Methylethylidene)-2,4-pentanedione was prepared from 2-chloro-2-nitropropane and 2,4-pentanedione according to a procedure described by Russell et al.[25] Bp: 60–80 °C (8 mmHg). Yield: 23%. ^1H NMR ($CDCl_3$): δ 1.96 (s, 6 H, $COCH_3$), 2.29 (s, 6 H, $C(CH_3)_2$). ^{13}C NMR (CD_3COCD_3): δ 23.9 ($C(CH_3)_2$), 32.3 ($COCH_3$), 143.5 (C=C), 148.4 (C=C), 201.8 (C=O). Anal. Calcd for $C_8H_{12}O_2$: C, 68.55; H, 8.63. Found: C, 67.92; H, 8.81. MS, *m/e* 140.20 (M^+; calcd 140.18).

Ethyl α-Isopropylideneacetoacetate. This compound was prepared from 2-chloro-2-nitropropane and ethyl acetoacetate according to the procedure described for the preparation of 3-(1-methylethylidene)-2,4-pentanedione. Bp: 87–88 °C (6 mmHg). Yield: 39%. ^1H NMR ($CDCl_3$): δ 1.30 (t, 3 H, CH_3), 1.97 (s, 3 H, $COCH_3$), 2.10 (s, 3 H, $C(CH_3)$), 2.30 (s, 3 H, $C(CH_3)$), 4.25 (q, 2 H, OCH_2). ^{13}C NMR ($C_6D_5CD_3$): δ 15.5 (CH_3), 24.1 ($C(CH_3)_2$), 31.5 ($COCH_3$), 61.8 (OCH_2), 134.1 (C=C), 153.4 (C=C), 167.1 (C=O), 200.3 (C=O). Anal. Calcd for $C_9H_{14}O_3$: C, 63.51; H, 8.29. Found: C, 64.09; H, 8.23. MS, *m/e* 170.15 (M^+; calcd 170.21).

Pentacoordinated Phosphorus Compounds. In order to avoid decomposition during handling and purification of the phosphoranes, they were prepared in situ in the NMR tubes by adding equivalent amounts of freshly distilled phosphite and the selected pentanedione to the deuteriated solvents. The tubes were flushed with dry Argon and sealed. After leaving them at room temperature for 10–14 days, ^{31}P NMR indicated the reactions to be complete. ^1H, ^{13}C, and ^{31}P NMR spectra were then recorded and are listed in Tables I and II (vide supra).

Line-Shape Analysis. The rate constant *k* was obtained for each temperature by simulation of the experimental spectrum. Analyzing the coupled two-site exchange patterns (with $J_{AB} = 0$), using the DNMR/3 program,[10] the simulated spectra for all the different temperatures were obtained. For each study at least nine different temperatures were used. The $\Delta G^{\ddagger}$ was obtained from a least-squares plot of ln (k/T) versus $1/T$, using the Eyring model. The calculated errors lie within ±0.5 kJ·mol^{-1}. The validity of the $\Delta G^{\ddagger}$ values has been tested by calculating them from the equation $\Delta G^{\ddagger} = 1.91 \times 10^{-2} T_c(9.973 + \log (T_c/\Delta\nu))$. An excellent agreement with the values obtained from the line-shape analysis was found (Table III, vide supra).

Acknowledgment. This investigation has been supported by the Netherlands Foundation for Chemical Research (SON) with financial aid from the Netherlands Organization for the Advancement of Pure Research (ZWO). We thank Dr. N. K. de Vries for recording the ^{13}C NMR spectra of compound **a**[7] and Dr. P. A. Leclercq for recording the mass spectra of the pentadiones.

Registry No. 1, 1091-15-2; **2a**, 115094-83-2; **2b**, 115094-86-5; **2c**, 115094-84-3; **2d**, 115117-26-5; **3a**, 115094-85-4; **3b**, 115094-87-6; **3c**, 115117-25-4; **3d**, 115094-88-7; PCl_3, 7719-12-2; cyclopentylmethyl alcohol, 3637-61-4; 2-methoxyethanol, 109-86-4; 3-(phenylmethylene)-2,4-pentanedione, 4335-90-4; 3-(1-methylethylidene)-2,4-pentanedione, 26187-41-7; ethyl α-isopropylideneacetoacetate, 35044-52-1; 2-chloro-2-nitropropane, 594-71-8; ethyl acetoacetate, 141-97-9; tris(tetrahydrofurfuryl) phosphite, 5971-30-2; tris(cyclopentylmethyl) phosphite, 115094-89-8; tris(2-methoxyethyl) phosphite, 4156-80-3.

(24) McEntee, M. E.; Pinder, A. R. *J. Chem. Soc.* **1957**, 4426.
(25) Russell, G. A.; Mudryk, B.; Jawdosiuk, M. *Synthesis* **1981**, 62.

A Single-Crystal ESR Study on Radicals Derived from *rac*- and *meso*-1,2-Dimethyl-1,2-diphenyldiphosphine Disulfide: Stereochemical Selection in Radical Formation

René A. J. Janssen,* Mark J. van der Woerd, Olav M. Aagaard, and Henk M. Buck

Contribution from the Department of Organic Chemistry, Eindhoven University of Technology, P.O. Box 513, 5600 MB Eindhoven, The Netherlands. *Received November 23, 1987*

Abstract: An ESR study on electron-capture phosphorus centered radicals trapped in single crystals of *rac*- and *meso*-1,2-dimethyl-1,2-diphenyldiphosphine disulfide (MePhP(S)P(S)MePh) is reported. The principal values and axes of the **g** and hyperfine coupling tensors of the radical anions are determined. It is shown that X irradiation of the two diastereoisomeric compounds results in completely different radical products. The racemate yields a radical product in which the extra electron is symmetrically distributed over the two phosphorus nuclei, whereas for the meso form exclusively asymmetric electronic configurations are detected.

For many years the formation and structure of free radicals, produced by ionizing radiation, has received much attention. Numerous ESR experiments have been performed to elucidate the principles that determine the electronic structure and molecular geometry of the formed doublet species. This has resulted in a detailed understanding of the role of the nucleus at the radical center and of the influence of the surrounding ligands. Stereochemical aspects, however, are not generally included in these analyses. In the present study we report the formation of phosphorus-centered radicals in single crystals of racemic (*R*,*R* and

0002-7863/88/1510-6001$01.50/0